厚生労働科学研究費補助金
難治性疾患等実用化研究事業(難治性疾患実用化研究事業)

小児重症拡張型心筋症への bridge-to-transplantation/recovery を目指した 骨格筋芽細胞シートの開発と実践

平成２６年度　総括研究報告書

研究代表者　澤　芳樹

平成２７（２０１５）年５月

目次

厚生労働科学研究補助金（難治性疾患等実用化研究事業(難治性疾患実用化研究事業)）
総括研究報告書

小児重症拡張型心筋症への bridge-to-transplantation/recovery を目指した骨格筋芽細胞シートの開発と実践

研究代表者
大阪大学大学院医学系研究科　教授　澤　芳樹

研究要旨
既に、成人の心不全患者に対して開発が進められている自己由来骨格筋芽細胞シート移植を、小児重症拡張型心筋症患者へ適応することを目的とする。小児患者に対する本再生細胞治療法の安全性と有効性を検証し、医師主導治験実施と保健医療化を目指し、小児重症心不全患者に対する新たな治療法を確立する。

研究分担者
宮川　繁
大阪大学大学院医学系研究科 特任准教授（常勤）
松山　晃文
大阪大学臨床医工学融合研究教育ｾﾝﾀｰ 招聘教授
早川　堯夫
近畿大学薬学総合研究所　所長

A. 研究目的

小児拡張型心筋症は予後不良な難治性疾患であり、重症例に対しては心臓移植が究極の治療である。2010 年に臓器移植法が改正されたものの、それ以後の小児ドナーからの臓器提供は未だに少なく、心臓移植の実施例は欧米諸国と比べると稀有である。そのため、心臓移植待機期間は長期間におよび、我が国では心臓移植に到達するまでの橋渡しとして、新たな治療法を開発する必要がある。

自己由来骨格筋芽細胞シート移植治療は、当科において既に成人の心不全患者に対する再生治療として開発してきた。本治療法を小児患者に対して応用することにより、小児重症心不全に対する新たな治療戦略を確立することが可能と考えられる。

本研究の目的は、小児重症拡張型心筋症に対する自己由来骨格筋芽細胞シート移植の安全性と有効性を検証し、医師主導治験・保険診療化を目指すことである。

B. 研究方法

1）幼若動物を用いた、骨格筋芽細胞シート移植における非臨床安全性試験

本治療法の医師主導治験を実施するため、非臨床安全性試験の追加試験を実施した。幼若ミニブタ虚血性心疾患モデルを作成し、骨格筋芽細胞シート移植前後での心室性不整脈の発生頻度を確認した。心電図解析の方法は、Medtronic 社製植込み型心電計 Reveal®をシート移植前に、モデル動物の前胸部に植込み、プロトコル治療終了後に心電計を取り出し不整脈に発生状況を検証した。

2）骨格筋芽細胞シート移植による小児重症心筋症患者に対する臨床研究

平成 25 年に厚生労働省より実施承認を受けた、小児重症心筋症に対する骨格筋芽細胞シート移植のヒト幹細胞臨床研究（HM1401 号）を実施した。プロトコルに沿って、患者選定ならびに 1 例の被験者登録とシート移植術を施行し、6 カ月のフォ

ローアップを終了した。

3）骨格筋芽細胞シート移植による小児重症拡張型心筋症患者に対する医師主導治験

前年度末（平成26年3月27日）に、医師主導治験を実施するための、薬事戦略相談（対面助言）をPMDAと行った。その結果を受け、医師主導治験実施のための準備を行った。

（倫理面への配慮）

1）動物実験においては、本学動物実験規程に従って行った。

2）臨床研究の実施に際しては、研究計画書、試験薬概要書、手順書など臨床研究に必要な文書は、「ヒト幹細胞を用いる臨床研究に関する指針」を遵守して作成し、院内ヒト幹細胞臨床研究審査委員会での承認を受けた。その後、厚生労働大臣の承認を受け実施を行った。本研究の対象は小児であるために、同意説明には十分に配慮を行い、容易な文章を用いて作成した補助文書（アセント）などを使用し、可能な限り患者本人への説明も十分に行ったうえで、代諾者へのinformed consentを行い、同意を得て実施した。

3）医師主導治験においては、各種法令・告示・通知に基づき実施し、研究計画書（プロトコール）に関してPMDAでの審査、院内治験審査委員会での承認を受け、再生医療新法に基づき実施を予定する。

C. 研究結果

1）幼若動物を用いた、骨格筋芽細胞シート移植における非臨床安全性試験

骨格筋芽細胞シート移植に伴う、重篤な有害事象として心室性不整脈の増悪が懸念されている。幼若ミニブタ虚血性心筋症モデルを用いた筋芽細胞シート移植において、治療前後での心室性不整脈の発生頻度、重症度に関して、有意な変化は認められなかった。

2）骨格筋芽細胞シート移植による小児重症心筋症患者に対する臨床研究

小児拡張型心筋症患者1例に対して、骨格筋芽細胞シート移植術を行い、プロトコルに沿って6カ月間のフォローアップを完遂した。フォローアップ期間中、シート移植治療が原因となる重篤な有害事象は認めなかった。左室収縮能は、増悪を認めず、拡張能に関しては軽度の改善を認めた。臨床症状の改善（NYHAⅢ度からⅡ度へ）と、6分間歩行において、運動耐容能の改善を認めた。

3）骨格筋芽細胞シート移植による小児重症拡張型心筋症患者に対する医師主導治験

前年度実施した対面助言の結果を受け、プロトコルの改正等を行って、平成26年6月16日フォローアップ面談を実施した。非臨床安全性試験を追加する必要がるということで助言を受け、前述の幼若動物を用いた、骨格筋芽細胞シート移植前後での心室性不整脈発生頻度について検証を行った。治験文書の作成、CROとの業務契約などを行い、院内IRB申請準備と実施体制の整備を行った。

D. 考察

非臨床安全性試験では、幼若動物においても懸念されていた骨格筋芽細胞シート移植後の心室性不整脈の増悪は認められなかった。既に実施されている成人患者に対する本治療法による臨床研究でも、シート移植前後での不整脈の増悪は認められず、その安全性は担保されつつある。小児患者に対する細胞シート移植後も、心室性不整脈が増悪しない可能性が示唆された。

臨床研究では、1例の小児拡張型心筋症患者に対して、本治療法が適応された。細胞シート移植後の6ヵ月フォローアップ期間中、重篤な有害事象は報告されず、安全性を示すことができた。本症例の経時的推移としては、心機能ならびに臨床症状の改善が認められ、有効性も示唆される所見が得られた。安全性及び有効性評価に関しては、さらなる症例数の蓄積が必要であり、今後も被験者選定とリクルートを継続する。

医師主導治験実施を予定しており、実施体制の整備と必要な安全性試験の実施を行うことができた。平成27年度以降、院内での治験審査委員会での承認、治験届の提出等、治験実施に向けての準備を継続する予定である。

E. 結論

本研究は、自己骨格筋芽細胞シート治療による新たな小児心不全治療体系の確立を目的として実施された。非臨床試験と臨床研究実施での本治療法の安全性が示唆されたため、今後、医師主導治験へと展開することが可能であり、保険診療化を目指した開発が進むものと思われる。

F. 健康危険情報

該当なし

G.研究発表

1．論文発表

1. Cell-sheet therapy with omentopexy promotes arteriogenesis and improves coronary circulation physiology in failing heart.
Kainuma S, Miyagawa S, Fukushima S, Pearson J, Chen YC, Saito A, Harada A, Shiozaki M, Iseoka H, Watabe T, Watabe H, Horitsugi G, Ishibashi M, Ikeda H, Tsuchimochi H, Sonobe T, Fujii Y, Naito H, Umetani K, Shimizu T, Okano T, Kobayashi E, Daimon T, Ueno T, Kuratani T, Toda K, Takakura N, Hatazawa J, Shirai M, Sawa Y. Mol Ther. 2015 Feb;23(2):374-86. doi: 10.1038/mt.2014.225. Epub 2014 Nov 25.

2. Targeted delivery of adipocytokines into the heart by induced adipocyte cell-sheet transplantation yields immune tolerance and functional recovery in autoimmune-associated myocarditis in rats.
Kamata S, Miyagawa S, Fukushima S, Imanishi Y, Saito A, Maeda N, Shimomura I, Sawa Y. Circ J. 2015;79(1):169-79. doi: 10.1253/circj.CJ-14-0840. Epub 2014 Nov 5.

3. Safety and Efficacy of Autologous Skeletal Myoblast Sheets (TCD-51073) for the Treatment of Severe Chronic Heart Failure due to Ischemic Heart Disease. Yoshiki Sawa, , Yasushi Yoshikawa, MD, Koichi Toda,; Satsuki Fukushima, Kenji Yamazaki, Minoru Ono, Yasushi Sakata, Nobuhisa Hagiwara, Koichirou Kinugawa, Shigeru Miyagawa, Circ J. 2014 2015;79(5):991-9 doi: 10.1253/circj.CJ-15-0243

H. 知的財産権の出願・登録状況（予定を含む）

１．特許取得　該当なし

２．実用新案登録　該当なし

３．その他　特記事項なし

別紙４

研究成果の刊行に関する一覧表

雑誌

発表者氏名	論文タイトル名	発表誌名	巻号	ページ	出版年
Kainuma S, Miyagawa S, Fukushima S, Pearson J, Chen YC, Saito A, Harada A, Shiozaki M, Iseoka H, Watabe T, Watabe H, Horitsugi G, Ishibashi M, Ikeda H, Tsuchimochi H, Sonobe T, Fujii Y, Naito H, Umetani K, Shimizu T, Okano T, Kobayashi E, Daimon T, Ueno T, Kuratani T, Toda K, Takakura N, Hatazawa J, Shirai M, Sawa Y.	Cell-sheet therapy with omentopexy promotes arteriogenesis and improves coronary circulation physiology in failing heart.	Mol Ther.	Feb;23(2)	374-86	2014Nov 25.
Kamata S, Miyagawa S, Fukushima S, Imanishi Y, Saito A, Maeda N, Shimomura I, Sawa Y.	Targeted delivery of adipocytokines into the heart by induced adipocyte cell-sheet transplantation yields immune tolerance and functional recovery in autoimmune-associated myocarditis in rats.	Circ J.	2015;79(1)	169-79	2015
Yoshiki Sawa, MD, PhD1, Yasushi Yoshikawa, MD, Koichi Toda, MD, PhD1; Satsuki Fukushima MD, PhD1, Kenji Yamazaki, MD, PhD2; Minoru Ono, MD, PhD3; Yasushi Sakata, MD, PhD4; Nobuhisa Hagiwara, MD, PhD5; Koichirou Kinugawa, MD, PhD6; Shigeru Miyagawa, MD, PhD1	Safety and Efficacy of Autologous Skeletal Myoblast Sheets (TCD-51073) for the Treatment of Severe Chronic Heart Failure due to Ischemic Heart Disease.	Circ J.	2015;79(5):	991-9	2015

Cell-sheet Therapy With Omentopexy Promotes Arteriogenesis and Improves Coronary Circulation Physiology in Failing Heart

Satoshi Kainuma[1], Shigeru Miyagawa[1], Satsuki Fukushima[1], James Pearson[2], Yi Ching Chen[2], Atsuhiro Saito[1], Akima Harada[1], Motoko Shiozaki[1], Hiroko Iseoka[1], Tadashi Watabe[3], Hiroshi Watabe[3], Genki Horitsugi[4], Mana Ishibashi[4], Hayato Ikeda[4], Hirotsugu Tsuchimochi[5], Takashi Sonobe[5], Yutaka Fujii[5], Hisamichi Naito[6], Keiji Umetani[7], Tatsuya Shimizu[8], Teruo Okano[8], Eiji Kobayashi[9], Takashi Daimon[10], Takayoshi Ueno[1], Toru Kuratani[1], Koichi Toda[1], Nobuyuki Takakura[6], Jun Hatazawa[4], Mikiyasu Shirai[5] and Yoshiki Sawa[1]

[1]Department of Cardiovascular Surgery, Osaka University Graduate School of Medicine, Osaka, Japan; [2]Monash Biomedical Imaging Facility and Department of Physiology, Monash University, Melbourne, Australia; [3]Department of Molecular Imaging in Medicine, Osaka University Graduate School of Medicine, Osaka, Japan; [4]Department of Nuclear Medicine and Tracer Kinetics, Osaka University Graduate School of Medicine, Osaka, Japan; [5]Department of Cardiac Physiology, National Cerebral and Cardiovascular Center Research Institute, Osaka, Japan; [6]Department of Signal Transduction, Research Institute for Microbial Diseases, Osaka University, Osaka, Japan; [7]Japan Synchrotron Radiation Research Institute, Harima, Japan; [8]Institute of Advanced Biomedical Engineering and Science, Tokyo Women's Medical University, Tokyo, Japan; [9]Division of Organ Replacement Research, Center for Molecular Medicine, Jichi Medical School, Tochigi, Japan; [10]Department of Biostatistics, Hyogo College of Medicine, Hyogo, Japan

Cell-sheet transplantation induces angiogenesis for chronic myocardial infarction (MI), though insufficient capillary maturation and paucity of arteriogenesis may limit its therapeutic effects. Omentum has been used clinically to promote revascularization and healing of ischemic tissues. We hypothesized that cell-sheet transplantation covered with an omentum-flap would effectively establish mature blood vessels and improve coronary microcirculation physiology, enhancing the therapeutic effects of cell-sheet therapy. Rats were divided into four groups after coronary ligation; skeletal myoblast cell-sheet plus omentum-flap (combined), cell-sheet only, omentum-flap only, and sham operation. At 4 weeks after the treatment, the combined group showed attenuated cardiac hypertrophy and fibrosis, and a greater amount of functionally ($CD31^+$/lectin$^+$) and structurally ($CD31^+$/α-SMA^+) mature blood vessels, along with myocardial upregulation of relevant genes. Synchrotron-based microangiography revealed that the combined procedure increased vascularization in resistance arterial vessels with better dilatory responses to endothelium-dependent agents. Serial ^{13}N-ammonia PET showed better global coronary flow reserve in the combined group, mainly attributed to improvement in the basal left ventricle. Consequently, the combined group had sustained improvements in cardiac function parameters and better functional capacity. Cell-sheet transplantation with an omentum-flap better promoted arteriogenesis and improved coronary microcirculation physiology in ischemic myocardium, leading to potent functional recovery in the failing heart.

Received 27 August 2014; accepted 16 November 2014; advance online publication 13 January 2015. doi:10.1038/mt.2014.225

INTRODUCTION

Heart failure following myocardial infarction (MI) is a major cause of death and disability worldwide. Despite advances in drug and device therapy, recovery of cardiac function and prevention of transition to heart failure in MI patients remain unsatisfactory, indicating the need for development of novel therapeutic alternatives.[1] Myocardial regenerative therapy with cell-sheet transplantation has been shown to induce angiogenesis via paracrine effects in a chronic MI model.[2,3] However, the proangiogenic effect of the stand-alone cell-sheet treatment may be insufficient to fully relief ischemia in the chronic MI heart that involves a large territory of the left ventricle (LV), since the coronary inflow of the ischemic/infarct myocardium is dependent upon collateral arteries from other territories.[4,5] In addition, microvascular dysfunction is present in critical chronic MI heart across a wide range of the peripheral coronary tree.[6] This highlights the need for a comprehensive understanding of the mechanism of angiogenesis induced by a cell-sheet therapy in ischemic hearts.

For successful therapeutic neovascularization of ischemic tissues, it is essential to induce robust angiogenic responses (angiogenesis), and establish functionally and structurally mature arterial vascular networks (arteriogenesis) that show long-term stability and control perfusion.[5] Establishment of mature vessels is a complex process that requires several angiogenic factors to stimulate vessel sprouting and remodeling (endothelial tubulogenesis accompanied with a pericyte recruitment) of the primitive vascular network. Endothelial vasodilator function of coronary microvessels (resistance arterial vessels) is also an important determinant of myocardial perfusion in response to increased myocardial oxygen demand, playing a critical role in neovascular therapies.[6–8] The attenuated therapeutic effects observed in the previous clinical trials were caused by multiple factors including

Correspondence: Yoshiki Sawa, Chairman of Department of Cardiovascular Surgery, Osaka University Graduate School of Medicine, 2-2-E1, Yamadaoka, Suita, Osaka 565–0871, Japan. E-mail: sawa-p@surg1.med.osaka-u.ac.jp

generation of unstable blood vessels that regress over time or functionally immature vessels accompanied with endothelial dysfunction in ischemic areas.[5,9]

The omentum (OM), historically used in surgical revascularization for patients with ischemic heart disease, is also known to release a number of angiogenic cytokines and attenuate inflammation.[10–14] In addition, the gastroepiploic artery involved in the OM-flap can play an important role as an extracardiac blood source with high perfusion capacity for developing effective collateral vessels for advanced coronary artery disease. We established a combination strategy of cell-sheet transplantation covered with a pedicle OM-flap in porcine models, allowing us to implant large numbers of cells and improve cell survival.[13,14] However, data are scarce regarding the therapeutic effects of such combined treatment on vessel maturity and coronary microcirculation physiology in ischemic territory. We hypothesized that cell-sheet transplantation with a pedicle OM-flap will better promote arteriogenesis and stabilize blood vessels in ischemic myocardium along with improved coronary microcirculation physiology, consequently enhancing the therapeutic effects of cell-sheet therapy. Herein, we focused on vessel maturation induced by cell-sheet therapy with an OM-flap and evaluated the physiological benefits in coronary microcirculation utilizing modern modalities such as *in vivo* synchrotron-based microangiography and positron emission tomography (PET).

RESULTS

Histological analysis of host myocardium

Four weeks after treatment, myocardial structural components, collagen accumulation and cardiomyocyte hypertrophy, were assessed by hematoxylin-eosin, Masson trichrome, and Periodic acid-Schiff staining ($n = 11$ for each group). LV myocardial structure was better maintained in the combined group as compared with the others (**Figure 1c**). The combined group had a significantly thickened anterior LV wall (anterior wall thickness, control 392 ± 31 versus combined 912 ± 34 versus sheet-only 688 ± 27 versus OM-only 500 ± 28 μm) (**Figure 1d**). That group also had a significantly attenuated collagen accumulation (percent fibrosis, 18 ± 1 versus 8 ± 4 versus 13 ± 6 versus 14 ± 1%, respectively) (**Figure 1e**) and cardiac hypertrophy (myocyte size, 23 ± 1 versus 16 ± 1 versus 20 ± 3 versus 21 ± 2 μm, respectively) (**Figure 1f**) in the peri-infarct regions (ANOVA $P < 0.001$ for all).

Gene expressions in peri-infarct myocardium during acute treatment phase

The myocardial gene expressions related to angiogenesis, vessel maturation, and anti-inflammation were analyzed at 3 days after each treatment using real-time PCR ($n = 6$ for each group). As compared to the others, the combined group showed substantially higher gene expressions of *vascular endothelial growth factor (VEGF)-A*, *VEGF receptor-1*, *VEGF receptor-2*, *Akt-1*, *platelet-derived growth factor (PDGF)-β*, *angiopoietin (Ang)-1*, *Tie-2*, *vascular endothelial (VE)-cadherin*, *platelet endothelial cell adhesion molecule (PECAM)-1*, and *stromal cell-derived factor (SDF)-1* in peri-infarct myocardium at the early stage of transplantation (**Figure 2**).

Vessel recruitment in transplanted cell-sheets and donor cell survial

To evaluate the effect of adding OM-flap to the cell-sheet therapy on the vessel recruitment (angiogenesis) in the transplanted area that should be related to the donor cell survival, we serially assessed the number of functional blood vessels with patent endothelial layers (CD31/lectin double-positive cells) in the transplanted area of the sheet-only and combined groups at 3, 7, and 28 days after each treatment ($n = 6$ for each group and each time point) (**Figure 3a–f**). At 3 days after treatment, in the sheet-only group, several blood vessels were just located at the border between the sheet and infarct area (**Figure 3a**), whereas a large number of functional vessels was detected proximal to the border between the cell-sheet and OM and within the sheet in the combined group (**Figure 3d**), suggesting that the cell-sheet received blood supply directly from the infarct myocardium and OM. Consequently, the combined group had greater numbers of functional blood vessels in the cell-sheet than the sheet-only group at any follow-up point, although both groups showed steady decrease in the number of vessels during the 28 days (**Figure 3g**).

The quantitative assessments of the donor (GFP-positive) cell presence were also serially performed to elucidate the donor cell dynamics in the sheet-only (**Figure 3a–c**) and combined (**Figure 3d–f**) groups. We traced the transplanted donor cells and found that there was no significant difference in the engrafted area at 3 days after transplantation between the groups, while the subsequent changes in each group were apparently distinctive (**Figure 3h**). During the 7days after the treatment, the amount of decrease in the engrafted area was substantially smaller in the combined group than that in the sheet-only group, resulting in 4.3-fold increased retention of donor cells in the former group. This led to the greater donor cell presence in the combined group persistently (at least until day 28), which was consistent with the amount of vessel recruitment in the cell-sheet.

Vessel remodeling and maturation in peri-infarct myocardium

We serially assessed neovascular vessel maturity in peri-infarct areas at 3 ($n = 6$ for each group) and 28 days ($n = 11$ for each group) after treatment (**Figure 4**). Vessel density and structural maturity were quantified as the number of CD31 positive and CD31/α-smooth muscle actin (SMA) double-positive vessels per mm^2, respectively. A maturation index was calculated as the percentage of CD31/α-SMA double-positive vessels to total vessel number. Functionally mature vessels with patent endothelial layers were assessed by lectin injection, which binds uniformly and rapidly to the luminal surface of endothelium, thus labeling patent blood vessels. Vessels positive for CD31 but negative for lectin were regarded as functionally immature and undergoing regression, or that had lost patency.[15,16]

In general, α-SMA signals were located at the outer edges of CD31 staining, indicating pericyte attachment to newly formed endothelium. Three days after treatment, there was no difference in number of CD31-positive cells among the groups, though the combined group showed a trend of greater number of functional blood vessels with patent endothelial layers (CD31/lectin double-positive) and structurally (CD31/α-SMA double-positive) mature vessels, with a higher maturation index (**Figure 4a–g**). Notably, the percentage without lectin staining ($CD31^+$/$lectin^-$) was significantly smaller in the combined group.

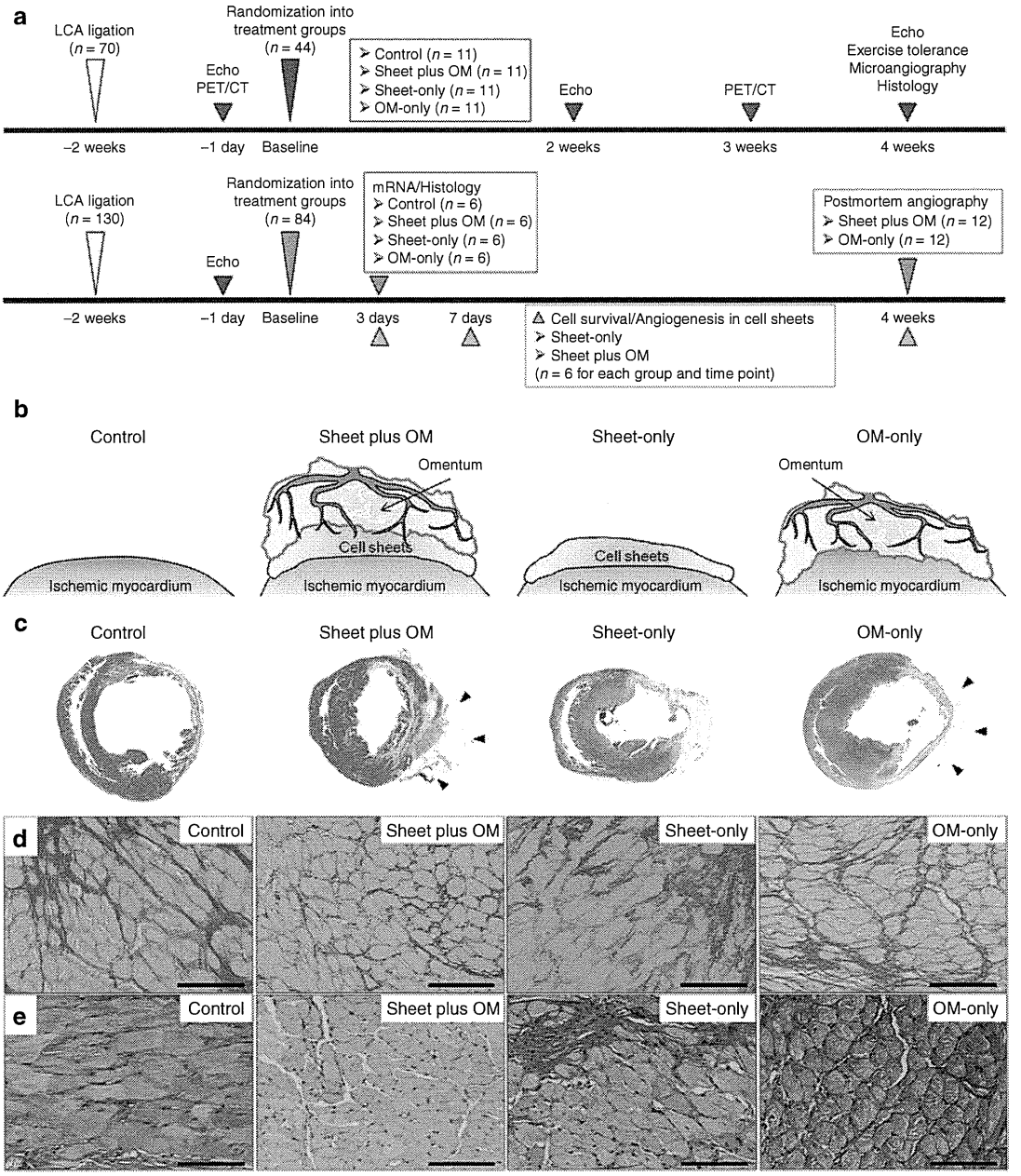

Figure 1 (**a**) Experimental protocols. (**b**) Procedural schemes for treatment groups. (**c**) Macroscopic images of HE-stained whole sections of the left ventricle and (**d**) anterior wall thickness (40×, scale bar = 1,000 μm). Black arrows indicate the omentum tissue. Photomicrographs of Sirius red- (**e**) and periodic acid-Schiff-stained (**f**) sections of peri-infarct myocardium (400×, scale bar = 100 μm) (n = 11 for each group).

The number of endothelial (CD31 positive) cells in the control and single treatment groups decreased with time, while that in the combined remained unchanged. Consequently, the angiogenic effects induced in the latter were more profound at 28 days after treatment, with a significantly greater amount of mature vessels (Figure 4h–n).

Number of resistance vessels and relative dilatory responses to endothelium-dependent stimulation in ischemic myocardium

To evaluate the effects of each treatment on microcirculation physiology in terms of relative dilatory responses to acetylcholine and dobutamine hydrochloride in the resistance vessels, synchrotron radiation microangiography was performed after 3 weeks after the treatment (control: n = 11, combined: n = 11, cell-sheet: n = 5, OM: n = 6). Using iodinated agents, coronary microcirculation in ischemic areas was clearly visualized in anesthetized closed-chest rats (Figure 5a). Vessel internal diameter (ID) at baseline (before agent administration) tended to decrease according to branching order and differed among the groups with larger first branching order arteries observed in the combined group (Figure 5b). Moreover, the combined group had a greater number of third and fourth branching order arterial vessels (resistance arterial vessels) at baseline (Figure 5c).

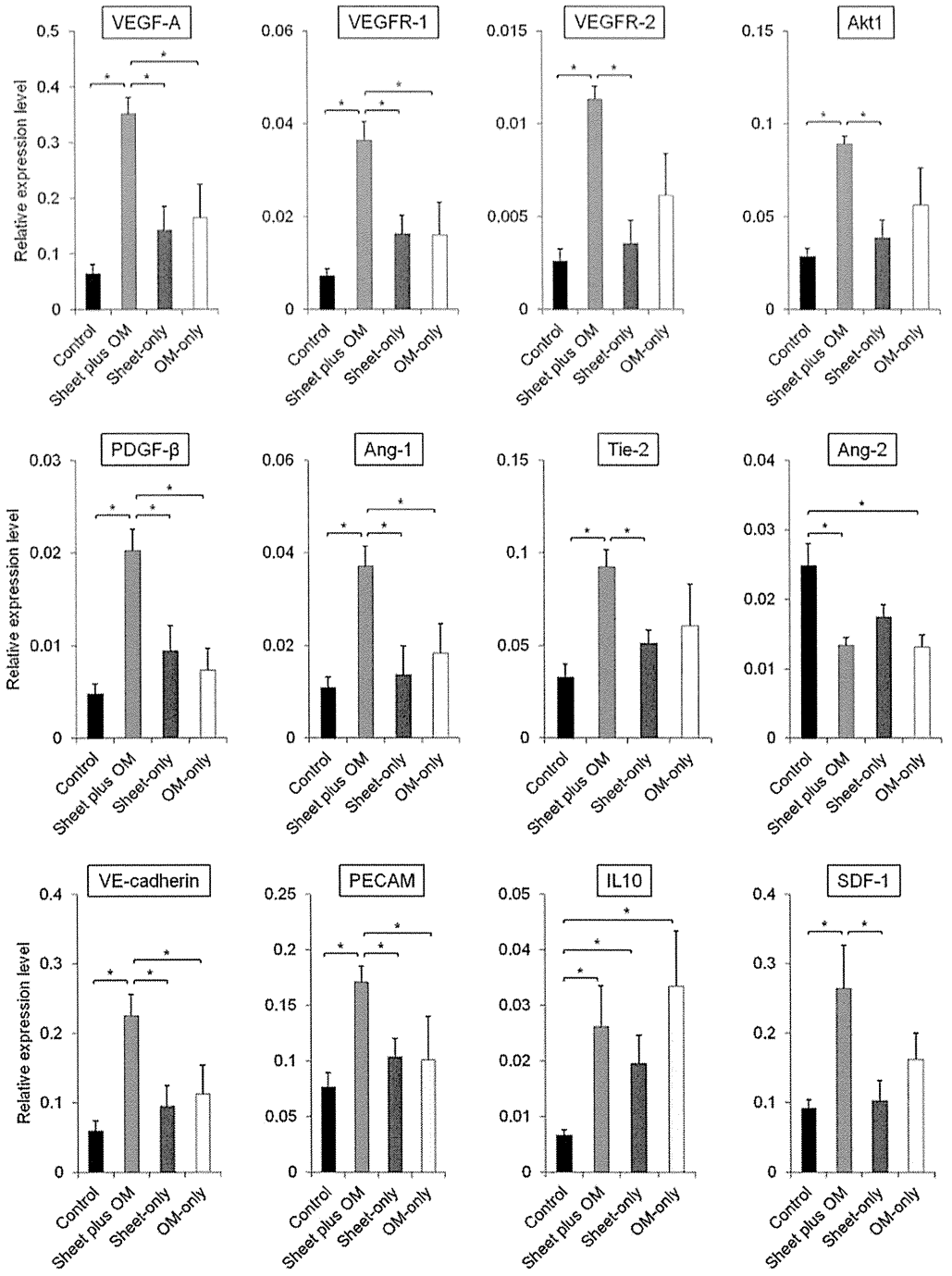

Figure 2 Quantitative reverse transcription PCR showing gene expressions related to angiogenesis, vessel maturation, and anti-inflammation in peri-infarct myocardium 3 days after treatment ($n = 6$ for each group) (*$P < 0.05$). Data were normalized to β-actin expression level. As compared to the others, the combined group showed substantially higher gene expressions associated with angiogenesis, vessel remodeling and anti-inflammation in peri-infarct myocardium at 3 days after treatment.

Acetylcholine-mediated dilation in the third and fourth branching orders was significantly different among the groups. The mean caliber changes in response to acetylcholine in the combined group were 28±8% and 32±8% for the third and fourth order branches respectively, which were greater than in the others (Figure 5d). Similarly, the mean caliber changes in response to dobutamine hydrochloride in the combined group were 31±7% and 34±7%, respectively, which were greater than in the others (Figure 5e).

The distributions of individual segment caliber changes in response to acetylcholine are described in **Supplementary Figure S1**. The control group had a relatively high frequency of third and fourth branching order arterial vessels showing localized segmental vasoconstriction (ID constriction >5% of baseline). The frequency of abnormal vasoconstriction with acetylcholine in the control group was about eight- and fourfold for the third and fourth branching order, respectively, as compared

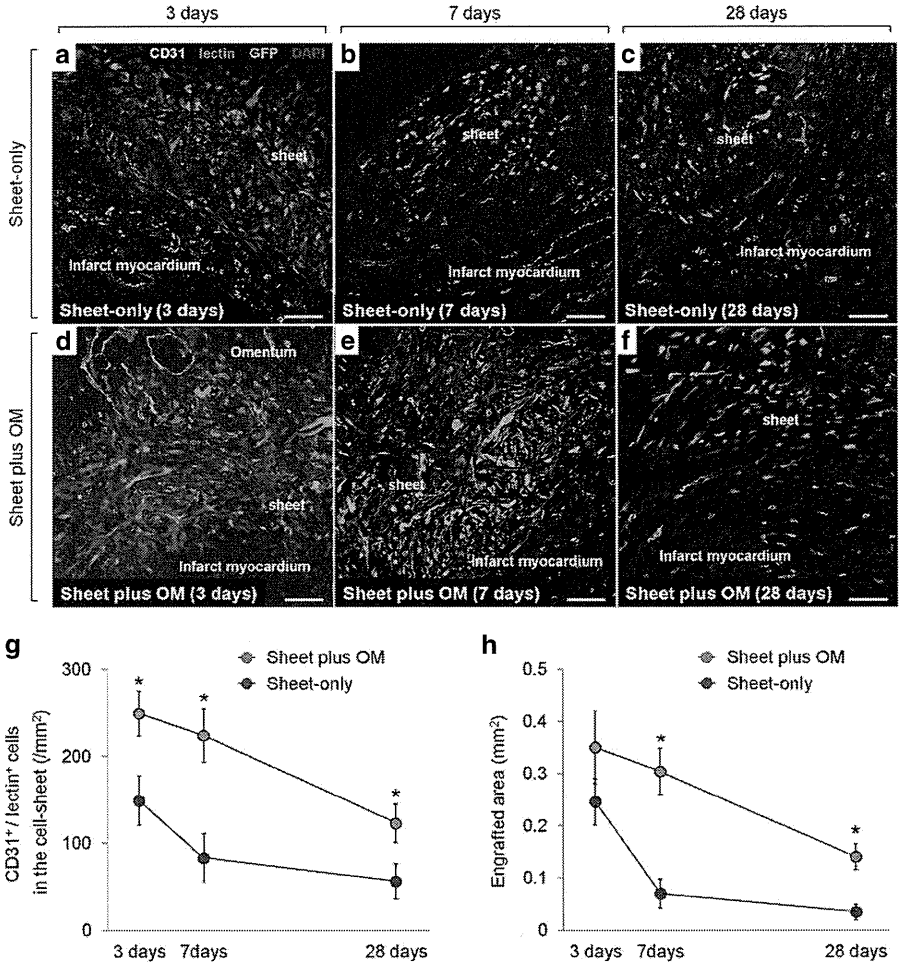

Figure 3 Serial representative images of functional blood vessels with patent endothelial layers (CD31/lectin double-positive) vessels in the transplanted donor (GFP-positive) cells in sheet-only (a–c) and combined groups (d–f) at 3, 7, and 28 days after each treatment (200×, scale bar = 100 μm). Quantitative analyses of functionally mature vessels in the transplanted area (**g**) and the donor (GFP-positive) cell presence (**h**) at 3, 7, and 28 days after each treatment ($n = 6$ for each group and each time point) (* $P < 0.05$ versus sheet-only group). At 3 days after treatment, in the sheet-only group, several blood vessels were just located at the border between the sheet and infarct area (**a**), whereas a large number of functional vessels was detected proximal to the border between the cell-sheet and OM and within the sheet in the combined group (**d**). Consequently, the combined group had greater numbers of functional blood vessels in the cell-sheet than the sheet-only group at any follow-up point (**g**). There was no significant difference in the engrafted area at 3 days after transplantation between the groups, while the subsequent changes in each group were apparently distinctive (**h**). During the 7 days after the treatment, the amount of decrease in the engrafted area was substantially smaller in the combined group than that in the sheet-only group, resulting in 4.3-fold increased retention of donor cells in the former group. This led to the greater donor cell presence in the combined group persistently (at least until day 28), which was consistent with the amount of vessel recruitment in the cell-sheet.

with the combined group (third order: control 49% versus combined 6% versus sheet-only 22% versus OM-only 25%; fourth order: control 18% versus combined 4% versus sheet-only 13% versus OM-only 17%).

Global and regional changes in myocardial blood flow and coronary flow reserve

To evaluate global and regional myocardial blood flow (MBF), and coronary flow reserve (CFR), ^{13}N-ammonia PET measurements were serially performed 1 day before and 3 weeks after the treatments (control: $n = 5$, combined: $n = 8$, cell-sheet: $n = 7$, OM: $n = 7$) (Figure 6a–f). In normal rats used for the validation study, global MBF at rest and during stress was 5.1 ± 0.5 and 7.1 ± 1.3 ml/min/g respectively, while global CFR was 1.4 ± 0.3.

Two weeks after coronary ligation (before treatment), global MBF at rest and during stress were substantially decreased in all groups, with no significant differences. Similarly, global CFR was not different among the groups. Three weeks after treatment, global MBF at rest was not different, while that during stress was significantly greater in the combined and single treatment groups as compared to the control (control 2.5 ± 0.4 versus combined 3.8 ± 0.6 versus sheet-only 3.3 ± 0.5 versus OM-only 3.8 ± 0.3, respectively, ANOVA p=0.0003). Postoperative global CFR was also substantially higher in the treatment groups as compared with the control (control 1.1 ± 0.2 versus combined 1.4 ± 0.2 versus sheet-only 1.4 ± 0.2 versus OM-only 1.4 ± 0.2, respectively, ANOVA p=0.015).

With regard to the magnitude of change in the global CFR (pre- versus post-treatment), the combined group offered the

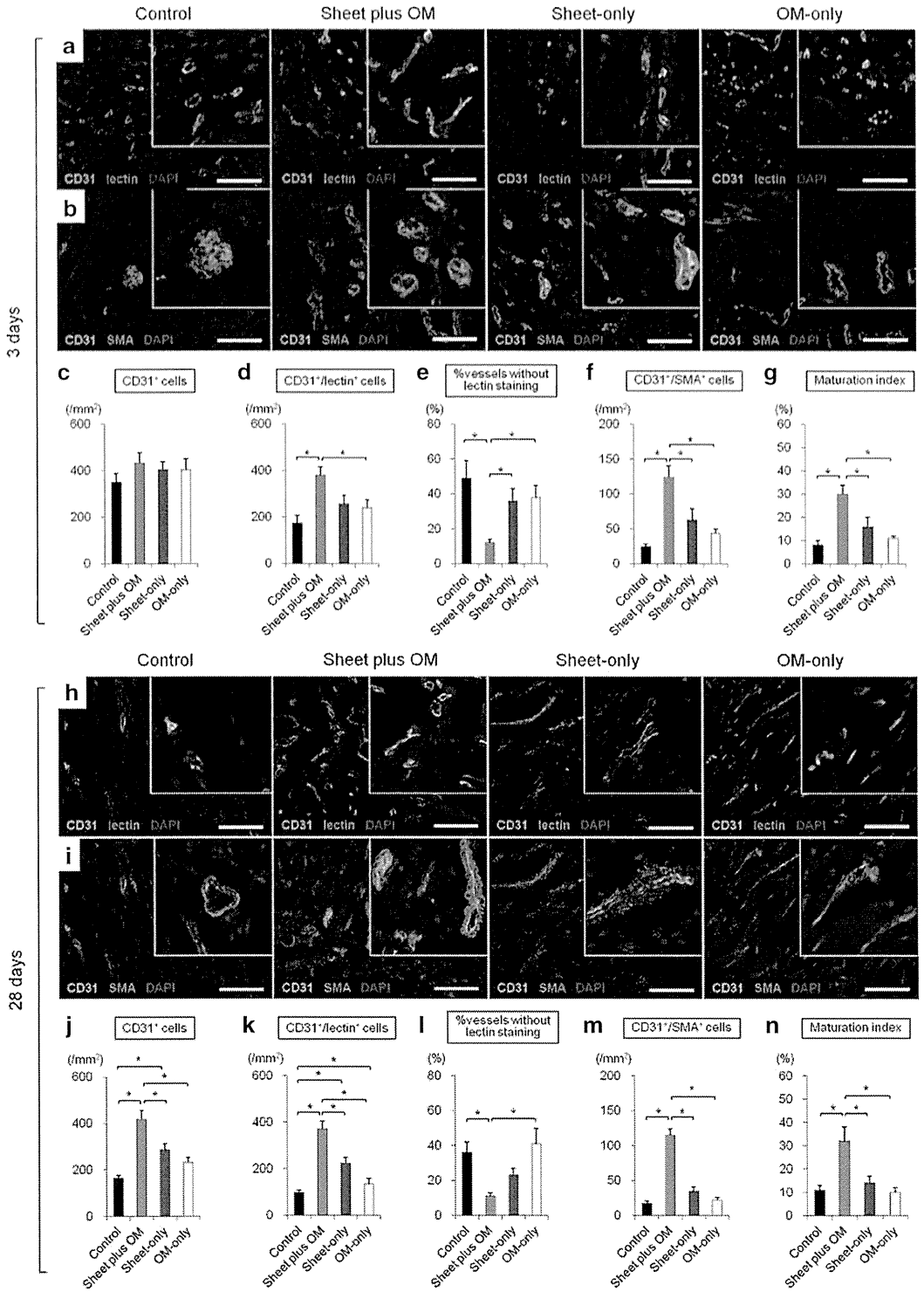

Figure 4 Immunohistochemical analyses of functionality (patency) and vessel maturation observed in peri-infarct myocardium at 3 ($n = 6$ for each group) (**a**–**g**) and 28 ($n = 11$ for each group) (**h**–**n**) days after treatments (* $P < 0.05$). Representative CD31/lectin and CD31/α-SMA staining at 3 (**a**,**b**) and 28 (**h**,**i**) days after treatments (400×, scale bar= 100 μm). Three days after treatment, there was no difference in number of CD31-positive cells among the groups, though the combined group showed a trend of greater number of functional blood vessels with patent endothelial layers (CD31/lectin double-positive) and structurally (CD31/α-SMA double-positive) mature vessels, with a higher maturation index (**c**–**g**). Notably, the percentage without lectin staining ($CD31^+/lectin^-$) was significantly smaller in the combined group. The number of endothelial (CD31 positive) cells in the control and single treatment groups decreased with time, while that in the combined remained unchanged. Consequently, the angiogenic effects induced in the latter were more profound at 28 days after treatment, with a significantly greater amount of mature vessels (**j**–**n**).

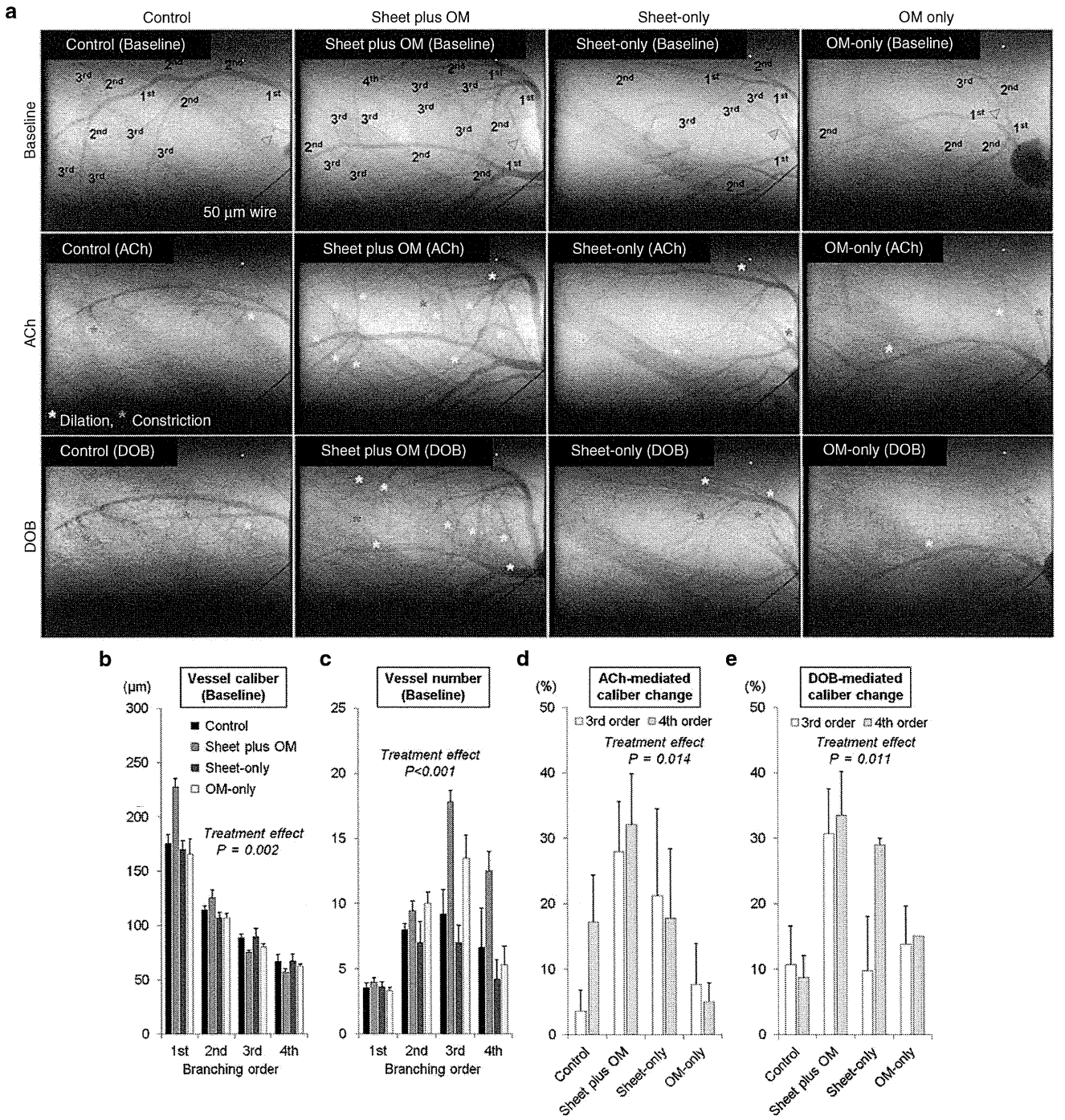

Figure 5 Synchrotron radiation microangiography was performed to evaluate vessel number and caliber and relative dilatory responses to acetylcholine and dobutamine hydrochloride in resistance vessels (control: $n = 11$, combined: $n = 11$, cell-sheet: $n = 5$, OM: $n = 6$). Using iodinated agents, coronary microcirculation in ischemic areas was clearly visualized in anesthetized closed-chest rats. Representative angiogram frames for all treatment groups at baseline, and in response to acetylcholine and dobutamine hydrochloride (**a**). Yellow and red asterisks indicate vessels showing dilation and constriction in response to acetylcholine and dobutamine hydrochloride, respectively. Quantitative analyses of (**b**) vessel internal diameter and (**c**) visible vessel number at baseline according to branching order. Vessel internal diameter at baseline (before agent administration) tended to decrease according to branching order and differed among the groups with larger first branching order arteries observed in the combined group (**b**). Moreover, the combined group had a greater number of third and fourth branching order arterial vessels (resistance arterial vessels) at baseline (**c**). Mean caliber changes in response to (**d**) acetylcholine and (**e**) dobutamine hydrochloride. Acetylcholine-mediated dilation in the third and fourth branching orders was significantly different among the groups. The mean caliber changes in response to acetylcholine in the combined group were 28 ± 8% and 32 ± 8% for the third and fourth order branches respectively, which were greater than in the others (**d**). Similarly, the mean caliber changes in response to dobutamine hydrochloride in the combined group were 31 ± 7% and 34 ± 7%, respectively, which were greater than in the others (**e**).

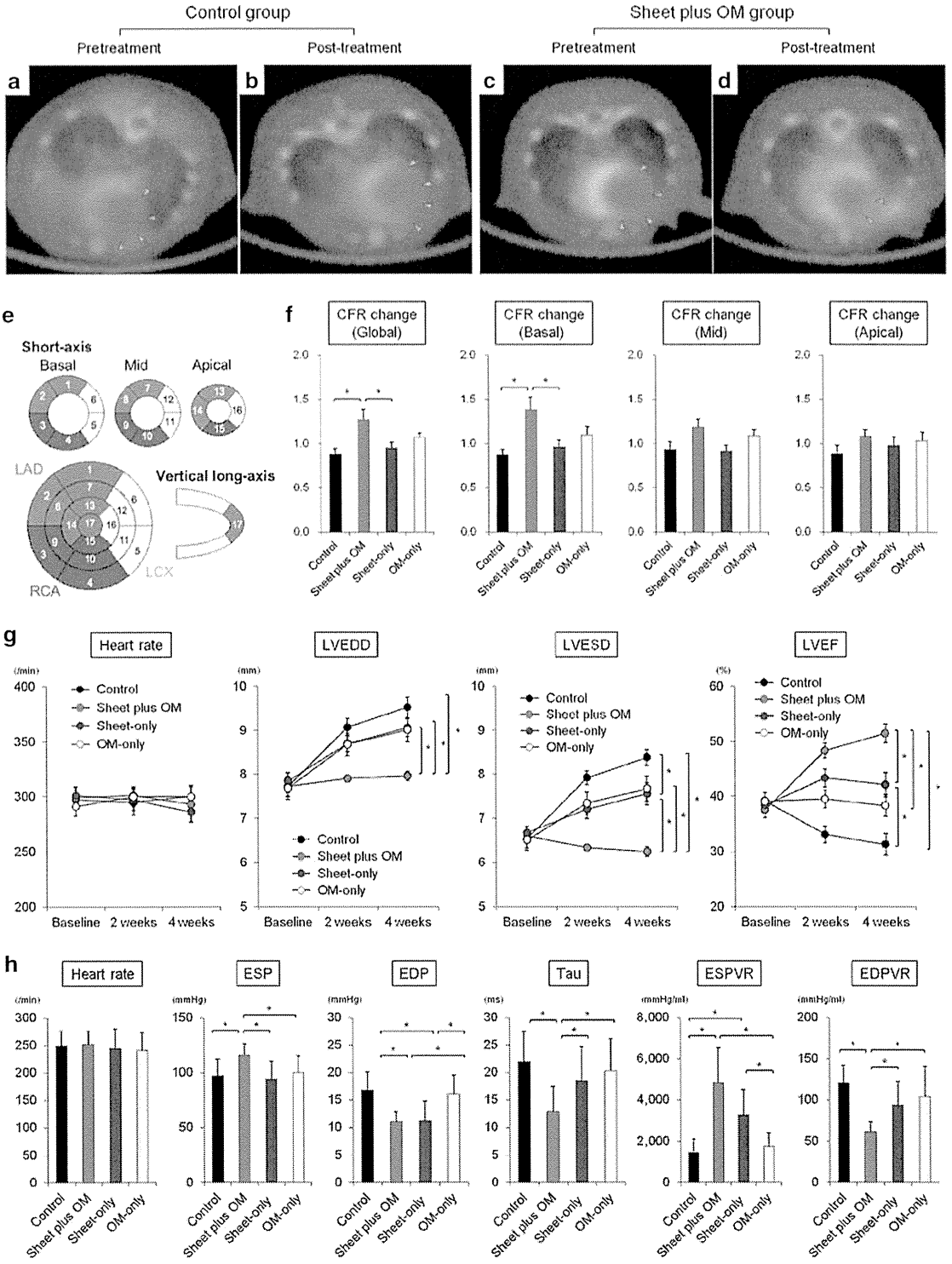

Figure 6 Representative serial PET/CT fusion images of ^{13}N-NH_3 PET during stress in control (a,b) and combined (c,d) groups. Recovery of MBF in large portion of basal left ventricle (anterior and lateral segments) was observed in the combined but not control group (green triangles). Quantitative analyses of changes in CFR calculated as a ratio of post-treatment to pretreatment CFR in global, basal, mid, and apical LV segments (control: $n = 5$, combined: $n = 8$, cell-sheet: $n = 7$, OM: $n = 7$) (*$P < 0.05$) (**e,f**). The combined group offered the most remarkable improvement in the global CFR, as evidenced by a higher ratio of post- to pretreatment CFR. Notably, that beneficial change was mainly caused by significant improvement in the basal left ventricle. CFR, coronary flow reserve; MBF, myocardial blood flow. (**g**) Serial assessments of cardiac function parameters at baseline (before treatment), and 2 and 4 weeks after treatments (*$P < 0.05$). In the combined group, remarkable improvements in LV function parameters occurred promptly and were sustained for up to 4 weeks, resulting in significantly smaller LV dimensions and greater LV ejection fraction as compared with other treatment groups. (**h**) Quantitative analyses of hemodynamic function parameters for each treatment (*$P < 0.05$). The basic hemodynamic indices revealed that LV end-systolic pressure was higher, whereas LV end-diastolic pressure and time constant were lower in the combined group as compared to the others. Pressure–volume loop analysis revealed that end-systolic pressure–volume relationship was higher, while end-diastolic pressure–volume relationship was lower in the combined group.

most remarkable improvement in the global CFR, as evidenced by a higher ratio of post- to pre-treatment CFR. Notably, that beneficial change was mainly caused by significant improvement in the basal left ventricle (control 0.9 ± 0.1 versus combined 1.4 ± 0.4 versus sheet-only 1.0 ± 0.1 versus OM-only 1.1 ± 0.1, respectively, ANOVA $P = 0.012$) (Figure 6e,f).

Global LV function and hemodynamic performance

The cardiac function was evaluated by echocardiography before (at baseline) and 2 and 4 weeks after each treatment ($n = 11$ for each group) (Figure 6 g,h). Two weeks after left coronary artery ligation, severe dilatation of the LV chamber and severe systolic dysfunction were observed, with no significant differences among the groups (Figure 6g). In the control, LV dimensions increased and LV ejection fraction deteriorated in a time-dependent manner, suggesting progressive LV remodeling. In the sheet-only and OM-only groups, LV ejection fraction initially improved, then tended to deteriorate in association with gradual LV dilatation. In the combined group, remarkable improvements in LV function parameters occurred promptly and were sustained for up to 4 weeks, resulting in significantly smaller LV dimensions and greater LV ejection fraction as compared with other treatment groups.

Consistently, the basic hemodynamic indices revealed that LV end-systolic pressure was higher, whereas LV end-diastolic pressure and time constant were lower in the combined group as compared to the others. Load-independent parameters assessed by pressure–volume loop analysis revealed that end-systolic pressure–volume relationship was higher, while end-diastolic pressure–volume relationship was lower in the combined group (Figure 6h). These results confirmed that cell-sheet therapy combined with OM-flap improved the therapeutic effects of single treatment group (cell-sheet only or OM-flap only) for the treatment of chronic MI.

Functional capacity assessment

There was no difference in running distance at 4 rpm (control 125 ± 15 versus combined 148 ± 9 versus sheet-only 133 ± 10 versus OM-only 135 ± 15 m, ANOVA $P = 0.63$) ($n = 11$ in each). In contrast, the combined group showed more improved functional capacity in terms of longer running distance at 8 rpm (54 ± 5 versus 178 ± 17 versus 81 ± 10 versus 76 ± 7 m, respectively, ANOVA $P < 0.001$).

Angiographic assessment of communication between coronary arteries and pedicle omentum

Communication between the coronary arteries and branches of the gastroepiploic artery in the OM specimens was evaluated using three different methods with a different series of OM-only and combined group animals ($n = 12$ in each) (Figure 1a).

A postmortem angiography examination from the aortic root was performed to verify antegrade flow from the OM into the heart in the combined and OM-only groups ($n = 4$ for each group). In the combined group, aortography revealed that the gastroepiploic artery branches feeding the OM expanded into the heart, and established several tight junctions between the native coronary arteries and OM (Figure 7a). In contrast, in the OM-only group, the gastroepiploic artery branches failed to penetrate the heart, accompanied by immature leaky collateral vessel formation between the coronary artery and OM, evidenced by considerable leakage of contrast agent (Figure 7b).

We selectively injected India ink into the celiac artery to visually and histologically confirm vessel communication between the pedicle OM and native coronary artery ($n = 4$ for each group). Numerous collaterals filled with India ink were clearly identified between the gastroepiploic artery and native coronary arteries in the combined group, while that was not seen in the OM-only group (data not shown) (Figure 7c–e). Histological analysis confirmed vessel communication between those in the combined group (Figure 7f,g).

Finally, a selective perfusion via aortic root and celiac artery using two different MICROFIL colors was performed ($n = 4$ for each group). In the combined group, MICROFIL solution injected in a retrograde manner into the aortic root (MV-117 Orange) was easily shown expanded into the OM to communicate with the gastroepiploic artery (Figure 7h). That solution injected into the celiac artery (MV-120 Blue) was also found to expand into the myocardium and communicated with native coronary arteries (Figure 7i). Those findings were not seen in the OM-only group (data not shown).

Vessel migration into cell-sheet from host myocardium and omentum

To further confirm whether the OM- and host myocardium-derived endothelial cells migrated toward the cell-sheet, we established two types of parabiotic pair models ($n = 4$ for each).

In parabiotic pairs of wild-type MI rats that received transplantation of cell-sheets labeled with Cell Tracker TM Orange CMTMR followed by coverage with a GFP-transgenic rat oriented pedicle OM, a large number of OM-derived endothelial cells (isolectin/GFP double-positive cells) had migrated toward the cell-sheet (Figure 8a–d). Similarly, in another parabiotic pair of GFP-transgenic MI rats that received cell-sheet transplantation covered with a wild-type rat oriented pedicle OM, a large number of host myocardium-derived endothelial cells (isolectin/GFP double-positive cells) had migrated toward the cell-sheet (Figure 8e–h).

Cell-sheet stimulated vascular cell migration

We performed an *in vitro* migration assay using HUVECs to evaluate the effects of skeletal myoblast cell-sheet derived growth factors on vessel recruitment (Figure 8i). The number of migrating cells was significantly greater in the 100% conditioned medium group, followed by the 10% conditioned medium and control groups, suggesting that SM cell-sheet derived growth factors stimulate vascular cell migration in a concentration-dependent manner (Figure 8j,k).

DISCUSSION

The major findings of this study can be summarized as follows. As compared to the single treatment groups, the cell-sheet plus OM group showed (i) improved donor cell retention along with amplified angiogenesis in the cell-sheet through the follow-up (at least day 28), (ii) attenuated cardiac hypertrophy and

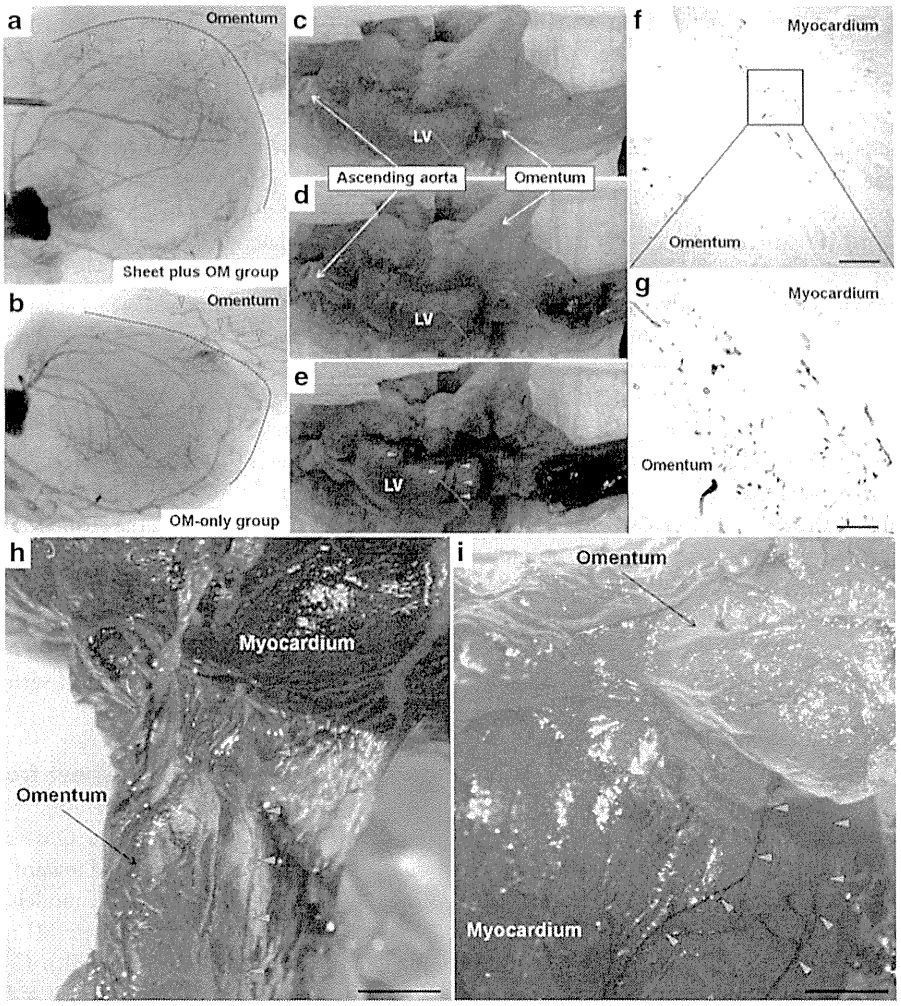

Figure 7 Communication between the coronary arteries and branches of the gastroepiploic artery was evaluated using three different methods with a different series of OM-only and combined group animals. A postmortem angiography examination from the aortic root in the combined (**a**) and OM-only (**b**) groups ($n = 4$ for each group). In the combined group, aortography revealed that the gastroepiploic artery branches feeding the OM expanded into the heart, and established several tight junctions between the native coronary arteries and OM (**a**). In contrast, in the OM-only group, the gastroepiploic artery branches failed to penetrate the heart, accompanied by immature leaky collateral vessel formation between the coronary artery and OM, evidenced by considerable leakage of contrast agent (red dotted circle) (**b**). Black dotted line indicates heart surface. Green triangles indicate the branches of the gastroepiploic artery. Selective India ink injection into the celiac artery to visually and histologically confirm vessel communication between the pedicle OM and native coronary artery ($n = 4$ for each group). Numerous collaterals filled with India ink were clearly identified between the gastroepiploic artery and native coronary arteries in the combined group (**c–e**), while that was not seen in the OM-only group (data not shown). Histological analysis confirmed vessel communication between those in the combined group (**f**: 40×, scale bar = 500 μm, **g**: 200×, scale bar = 100 μm). A selective perfusion via aortic root and celiac artery using two different MICROFIL colors ($n = 4$ for each group). In the combined group, MICROFIL solution injected in a retrograde manner into the aortic root (MV-117 Orange) was easily shown expanded into the OM to communicate with the gastroepiploic artery (**h**, 7.5×, scale bar = 2 mm). That solution injected into the celiac artery (MV-120 Blue) was also found to expand into the myocardium and communicated with native coronary arteries (**i**, 7.5×, scale bar = 2 mm). Those findings were not seen in the OM-only group (data not shown). Green triangles show visible vessel communication in the OM-flap (**h**) and host myocardium (**i**).

fibrosis, and a greater amount of functionally and structurally mature blood vessels in the ischemic myocardium, along with myocardial upregulation of relevant genes, (iii) increased vascularization in resistance arterial vessels with better dilatory responses to endothelium-dependent agents, (iv) more remarkable improvement in the global CFR, mainly caused by significant improvement in the basal left ventricle, (v) sustained improvements in cardiac function parameters and better functional capacity, and (vi) creation of robust vascular communication between the OM and native coronary arteries, shown by *in vivo* angiography.

The retention, survival, and engraftment of transplanted cells in the cell-sheet therapy are largely influenced by the degree of vascularization in the transplanted area and subsequent myocardial inflammation after cell-sheet transplantation.[2,17] The concept of combining OM-flap with the current cell-sheet therapy is likely to be reasonable because the OM is known to play a key role in controlling the spread of inflammation, and promoting revascularization, reconstruction and tissue regeneration. Our data suggest that the combined treatment improved the hypoxic environment in the transplanted area to a greater degree, potentially enhancing initial cell engraftment and enhancing the paracrine

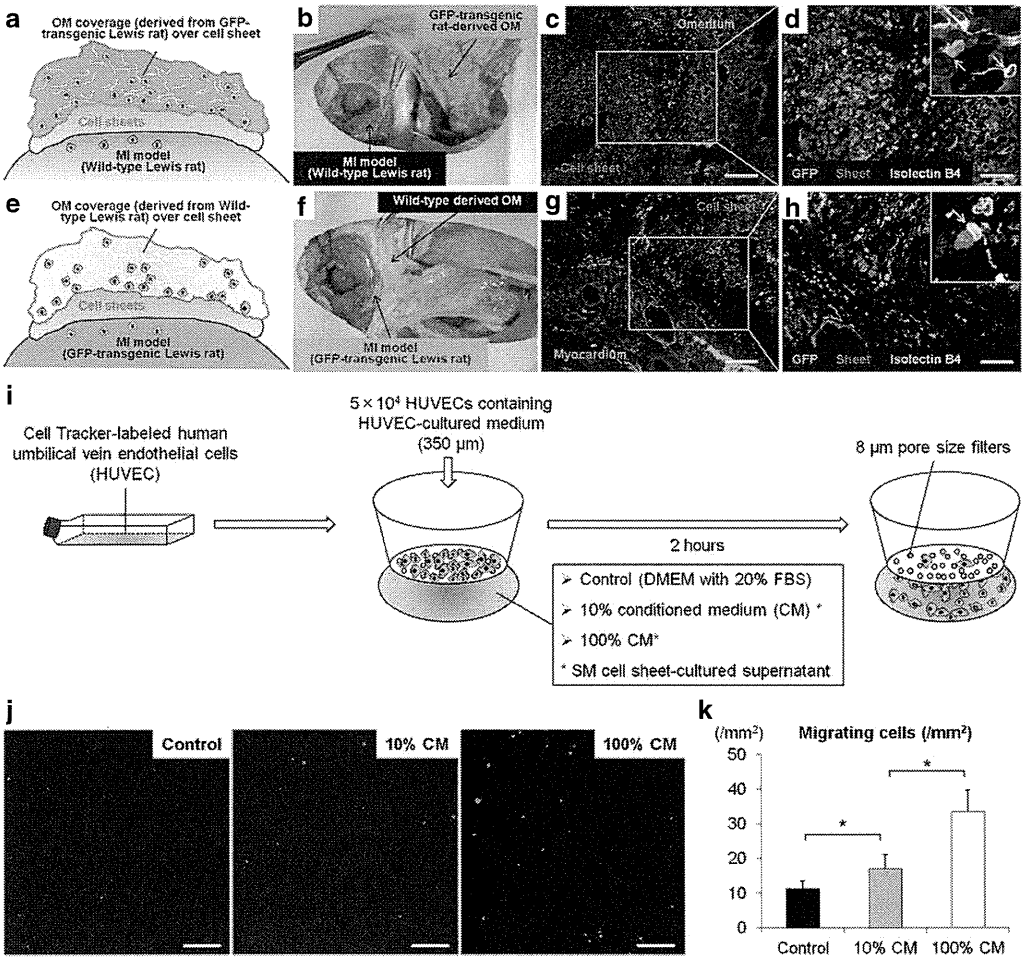

Figure 8 Schematic representation of experimental design to form parabiotic pairs of wild-type MI model rats (recipient) for transplantation of wild-type oriented cell-sheets labeled with Cell Tracker TM Orange CMTMR, followed by coverage with pedicle OM derived from GFP-transgenic rat (donor) (**a**,**b**). Representative GFP/isolectin staining in parabiotic pairs model (**c**: 100×, scale bar = 200 μm, **d**: 200×, scale bar = 100 μm). Schematic representation of experimental design to form second parabiotic pairs of GFP-transgenic MI rats for cell-sheet transplantation covered with wild-type oriented pedicle OM (**e**,**f**). Representative GFP/isolectin staining in second parabiotic pairs (**g**: 100×, scale bar = 200 μm, **h**: 200×, scale bar = 100 μm). *In vitro* migration assay (**i**). To investigate cell migration in response to skeletal myoblast cells cultured in conditioned medium, a modified Boyden chamber migration assay was performed using an HTS FluoroBlok Multiwell Insert System containing filters with a pore size of 8 μm. Human umbilical vein endothelial cells (HUVECs) were grown in EGM-2 culture medium. After incubation at 37 °C for 2 hours, the number of migrated cells was counted in 15 randomly chosen fields under 100× magnification using fluorescence microscopy. Two replicate samples were used in each experiment, which were performed at least twice. Migrating cells were analyzed using a light microscope and reported as numbers of migrating cells per mm² (**j**). Representative images show migrating cells labeled with Cell Tracker TM Orange CMTMR (100×, scale bar = 200 μm). Quantitative analyses of migrating cells according to concentration in the skeletal myoblast-cultured conditioned medium (**k**). Asterisk indicates statistical significance ($P < 0.05$).

effects induced by cell-sheet therapy in terms of higher expressions of relevant genes, potentially stabilizing therapeutic effect of cell-sheet therapy. The discrepancy between functional improvement and donor cell engraftment suggests that the improvement of cardiac function is not mainly mediated by direct contribution of transplanted donor cells but other indirect roles, possibly paracrine effects, offered by the cell-sheet at the early stage of transplantation.

The histological findings demonstrated that the rats receiving the cell-sheet implantation plus OM-flap had a significantly thickened anterior LV wall that was augmented by cardiomyocyte layers as compare to the other groups. Potential mechanisms may include cardiomyogenic differentiation of the donor-derived cells or endogenous stem cells, or paracrinal inhibition of progressive necrosis and/or apoptosis of the native cardiomyocytes. We speculate that both mechanisms might have contributed to the thickening of the targeted LV wall, although cardiomyogenic differentiation was not clearly identified in this study. Improved regional blood flow by the combined therapy could reduce the number of the necrotic/apoptotic cardiomyocytes, while reduced accumulation of fibrous components would inhibit thinning of the LV wall.[5,18] In addition, girdling effects from the covered OM might have reduced wall stress of the LV, leading to maintenance of the LV thickness.[19] Further studies to focus on the cardiomyogenic transdifferentiation using genetically labeled rodent models are warranted.

When blood vessels grow, endothelial cells migrate out first and assemble in a primitive network of immature channels

(angiogenesis).[5] As these nascent vessels only consist of endothelial cells, they rupture easily and are leaky, prone to regression, and poorly perfused.[18,20–22] Recruitment of mural cells around nascent vessels essentially contributes to remodeling and maturation of the primitive vascular network (arteriogenesis), subsequently causing therapeutic improvement of blood perfusion.[5,18] We found a larger percentage of vessels without lectin staining and lower maturation index in the control and single treatment groups, indicating that promotion of angiogenesis, but failure to effectively induce arteriogenesis. Consequently, the single treatments showed only transient effects on global cardiac function and limited functional capacity, possibly due to irregular capillary networks and increased vascular permeability. In the combined treatment group, greater numbers of functionally and structurally mature vessels were established promptly after treatment and maintained in ischemic myocardium. This might be primarily attributed to upregulated expressions of genes related to angiogenesis (*VEGF*, *VEGFR-1*, *VEGF-R2, Akt-1*) and/or endogenous regeneration (*SDF-1*). Moreover, elevated expressions of *Ang-1* and its receptor *Tie-2*, and *PDGF, VE-cadherin*, and *PECAM* might play key roles in promoting maturation processes such as "stabilization" of cell junctions and tight pericyte recruitment (arteriogenesis).[5,15,16,18,20–22] Interestingly, the elevated expression of the those relevant genes shown in the combined group was mostly reduced after 28 days after treatment (data not shown), corresponding with reduced donor cell presence. We found, however, the combined treatment group showed more sustained positive effects on vessel maturity and cardiac function recovery as compared with the control and single treatment groups at 28 days after treatment, indicating that paracrine mediators contribute to the myocardial recovery mainly during the early phase after the treatment and the effects on cardiac function and vessel structure, once established, could last for a longer time.[2] These data suggest that OM-flap covering the cell-sheet played a key role in accomplishing the maturity of the new vessels in the targeted myocardial territory, leading to formation of more organized and durable vascular network, as compared to the control and the single treatment groups.

Endothelial vasodilator function of coronary microvessels (resistance arterial vessels) is an important determinant of myocardial perfusion in response to increased myocardial oxygen demand, playing a critical role in neovascular therapies.[6–8] Vasodilation in response to specific endothelium-dependent and endothelium-independent stimuli within the coronary circulations can be measured to assess endothelial function. To the best of our knowledge, this is the first to verify that cell-sheet treatment with and without OM-flap could improve endothelial vasodilator function of resistance arterial vessels in a rat MI model, utilizing *in vivo* synchrotron-based microangiography that has proved an effective method for clearly visualizing resistance arterioles and accurately identifying neurohumoral modulation of coronary blood flow within the microcirculation for assessing therapy efficacy.[7,23,24] Microangiography revealed attenuated dilatation and a strong trend toward increased incidence of paradoxical constrictions in the control, followed by the single treatment group, suggesting that the endothelial-dependent vasodilator function in resistance arterial vessels was progressively impaired in those groups.[25,26] In contrast, combined treatment effectively restored endothelial function in resistance arterial vessels, evidenced by better dilatory responses to acetylcholine, an endothelium-dependent vasodilator.[27] This corresponds with PET/CT findings demonstrating substantial improvement in CFR, which indicated the ability of the myocardium to increase blood flow in response to increasing myocardial oxygen demand. Adenosine causes vasodilation by stimulating receptors in the microcirculation, facilitating measurement of the endothelium-independent CFR in the microcirculation. Interestingly, a remarkable improvement in CFR was observed in basal, but not apical LV, indicating that the combined treatment might be capable of improving microvasculature functionality of hibernating myocardium, rather than scar cardiac tissue. These physiological benefits in the coronary microcirculation may activate collateral growth through increased flow and shear stress, a powerful driving force of arteriogenesis, leading to enhanced functional capacity under a high load.[28,29] Therefore, we speculate that the present combined treatment strategy has potential to effectively prevent progression of endothelial dysfunction, which independently predicts major clinical adverse events in patients with heart failure.[28–30]

Our data suggest that the combination of cell sheet transplantation and OM-flap acts synergistically, rather than additively, on vessel maturation, coronary microcirculation physiology, functional capacity, and cardiac reverse remodeling, whereas the OM-only strategy failed to stabilize its long-term effect. These results encouraged us to investigate the role of the cell-sheet transplantation in activating the effects of OM-flap. Postmortem angiography findings demonstrated visible collateral vessels between the native coronary arteries and OM-flap in the combined group, whereas no tight junctions were shown in the OM-only group, indicating that formation of collateral vessels between native coronary arteries and OM was accelerated by the interposed cell-sheets. The possible mechanism of those findings might be explained by our *in vitro* migration assay demonstrating that growth factors and cytokines secreted by the cell-sheet stimulate migration of endothelial cells derived from both host myocardium and the OM toward the sheet, subsequently establishing robust vessel connections with persistent blood flow between the native coronary arteries and OM. In contrast, in the OM-only group, lack of that process caused immature leaky collateral vessel formation and thus inadequate collateral blood flow in the ischemic myocardium. Based on those findings, we speculate that the therapeutic effects of the combined treatment strategy might be responsible for increased donor cell survival and stimulation of donor cells induced by OM-flap as well as for cell-sheet–mediated activation of OM-flap as a donor artery with high perfusion capacity. Nevertheless, further studies are absolutely needed to determine the main molecular mechanism of therapeutic effects induced by the combined treatment.

LIMITATIONS

Considering the potential molecular mechanisms behind the beneficial histological and physiological alterations observed with the combined strategy, we found that a group of possibly relevant molecules including *VEGF-A*, *VEGF receptor-1*, *VEGF receptor-2*, *Akt-1*, *SDF-1*, *PDGF-β*, *Ang-1*, *Tie-2*, *VE-cadherin*, and *PECAM* were upregulated in the combined group, suggesting that the

effects may be attributed to activation of several paracrine molecules, rather than a single molecule. Although some may argue what kinds of cytokines play a major role in generating therapeutic effects among the many complex molecular and cellular mechanisms involved, we consider that establishment of mature vessels is a complex process that is not regulated by specific factors, but rather numerous multiple factors that also dynamically change in response to the process of angiogenesis or vessel maturation. We believe that use of a cell-sheet and pedicle-OM as synergistic intelligent engineered tissues can efficiently support the regenerative process by dynamic cross-talk with ischemic cardiac tissue.

Although we did not experience any complication such as torsion of omentum flap or diaphragmatic hernia in the rats receiving the combined treatment, it is considered that a conventional lapalotomy itself may adversely affect general conditions particularly in critically-ill heart failure patients. An endoscopic approach may be useful in minimizing the OM-flap procedure-related complications in clinical settings.

CONCLUSION

We demonstrated that cell-sheet transplantation with an omentum-flap better promoted arteriogenesis and improved coronary microcirculation physiology in ischemic myocardium tissue, leading to potent functional recovery in a rat MI model. Further development of this treatment strategy toward clinical application is encouraged.

MATERIALS AND METHODS

All experimental procedures were approved by an institutional ethics committee. Animal care was conducted humanely in compliance with the Principles of Laboratory Animal Care formulated by the National Society for Medical Research and the Guide for the Care and Use of Laboratory Animals, prepared by the Institute of Animal Resources and published by the National Institutes of Health (publication no. 85-23, revised 1996).

Two weeks after left coronary artery ligation, rats were divided into four groups: (i) skeletal myoblast cell-sheet transplantation covered with an OM-flap (combined group), (ii) cell-sheet transplantation only, (iii) OM-flap only, and (iv) sham operation (control group). The protocol of this study is shown in Figure 1a,b. All *in vivo* and *in vitro* assessments were carried out in a blinded manner. A detailed description of all methods and reagents used for the experiments is provided in the **Supplementary Materials and Methods**.

SUPPLEMENTARY MATERIAL

Figure S1. Frequency distribution charts showing individual segment caliber changes in response to acetylcholine in **(a)** third and **(b)** fourth branching order vessels.
Materials and Methods.

ACKNOWLEDGMENTS

We thank Tsuyoshi Ishikawa, Yuuka Fujiwara, Yuka Kataoka, Hiromi Nishinaka, Toshika Senba, and staff of the PET Molecular Imaging Center for their excellent technical assistance. This research was supported by Research on Regenerative Medicine for Clinical Application from the Ministry of Health, Labour and Welfare of Japan and the Australian Synchrotron International Synchrotron Access Program (ISAP AS-IA111). Experiments were performed at the Japan Synchrotron Radiation Research Institute (SPring-8, BL28B2, Proposal 2011A1169). T.S. is a consultant for CellSeed, Inc., and T.O. is an Advisory Board Member of CellSeed, Inc. and an inventor/developer holding a patent for temperature-responsive culture surfaces. The authors have no conflicts of interest to report.

REFERENCES

1. Shah, AM and Mann, DL (2011). In search of new therapeutic targets and strategies for heart failure: recent advances in basic science. *Lancet* **378**: 704–712.
2. Narita, T, Shintani, Y, Ikebe, C, Kaneko, M, Harada, N, Tshuma, N *et al.* (2013). The use of cell-sheet technique eliminates arrhythmogenicity of skeletal myoblast-based therapy to the heart with enhanced therapeutic effects. *Int J Cardiol* **168**: 261–269.
3. Sekiya, N, Matsumiya, G, Miyagawa, S, Saito, A, Shimizu, T, Okano, T *et al.* (2009). Layered implantation of myoblast sheets attenuates adverse cardiac remodeling of the infarcted heart. *J Thorac Cardiovasc Surg* **138**: 985–993.
4. Habib, GB, Heibig, J, Forman, SA, Brown, BG, Roberts, R, Terrin, ML *et al.* (1991). Influence of coronary collateral vessels on myocardial infarct size in humans. Results of phase I thrombolysis in myocardial infarction (TIMI) trial. The TIMI Investigators. *Circulation* **83**: 739–746.
5. Carmeliet, P and Jain, RK (2011). Molecular mechanisms and clinical applications of angiogenesis. *Nature* **473**: 298–307.
6. Gutiérrez, E, Flammer, AJ, Lerman, LO, Elízaga, J, Lerman, A and Fernández-Avilés, F (2013). Endothelial dysfunction over the course of coronary artery disease. *Eur Heart J* **34**: 3175–3181.
7. Shirai, M, Schwenke, DO, Tsuchimochi, H, Umetani, K, Yagi, N and Pearson, JT (2013). Synchrotron radiation imaging for advancing our understanding of cardiovascular function. *Circ Res* **112**: 209–221.
8. Furchgott, RF and Zawadzki, JV (1980). The obligatory role of endothelial cells in the relaxation of arterial smooth muscle by acetylcholine. *Nature* **288**: 373–376.
9. Banquet, S, Gomez, E, Nicol, L, Edwards-Lévy, F, Henry, JP, Cao, R *et al.* (2011). Arteriogenic therapy by intramyocardial sustained delivery of a novel growth factor combination prevents chronic heart failure. *Circulation* **124**: 1059–1069.
10. O'Shaugnessy, L (1937). Surgical treatment of cardiac ischemia. *Lancet* **232**: 185–194.
11. Takaba, K, Jiang, C, Nemoto, S, Saji, Y, Ikeda, T, Urayama, S *et al.* (2006). A combination of omental flap and growth factor therapy induces arteriogenesis and increases myocardial perfusion in chronic myocardial ischemia: evolving concept of biologic coronary artery bypass grafting. *J Thorac Cardiovasc Surg* **132**: 891–899.
12. Shrager, JB, Wain, JC, Wright, CD, Donahue, DM, Vlahakes, GJ, Moncure, AC *et al.* (2003). Omentum is highly effective in the management of complex cardiothoracic surgical problems. *J Thorac Cardiovasc Surg* **125**: 526–532.
13. Shudo, Y, Miyagawa, S, Fukushima, S, Saito, A, Shimizu, T, Okano, T *et al.* (2011). Novel regenerative therapy using cell-sheet covered with omentum flap delivers a huge number of cells in a porcine myocardial infarction model. *J Thorac Cardiovasc Surg* **142**: 1188–1196.
14. Kawamura, M, Miyagawa, S, Fukushima, S, Saito, A, Miki, K, Ito, E *et al.* (2013). Enhanced survival of transplanted human induced pluripotent stem cell-derived cardiomyocytes by the combination of cell sheets with the pedicled omental flap technique in a porcine heart. *Circulation* **128**(11 Suppl 1): S87–S94.
15. Mancuso, MR, Davis, R, Norberg, SM, O'Brien, S, Sennino, B, Nakahara, T *et al.* (2006). Rapid vascular regrowth in tumors after reversal of VEGF inhibition. *J Clin Invest* **116**: 2610–2621.
16. Inai, T, Mancuso, M, Hashizume, H, Baffert, F, Haskell, A, Baluk, P *et al.* (2004). Inhibition of vascular endothelial growth factor (VEGF) signaling in cancer causes loss of endothelial fenestrations, regression of tumor vessels, and appearance of basement membrane ghosts. *Am J Pathol* **165**: 35–52.
17. Shimizu, T, Sekine, H, Yang, J, Isoi, Y, Yamato, M, Kikuchi, A *et al.* (2006). Polysurgery of cell sheet grafts overcomes diffusion limits to produce thick, vascularized myocardial tissues. *FASEB J* **20**: 708–710.
18. Carmeliet, P and Conway, EM (2001). Growing better blood vessels. *Nat Biotechnol* **19**: 1019–1020.
19. Hagège, AA, Vilquin, JT, Bruneval, P and Menasché, P (2001). Regeneration of the myocardium: a new role in the treatment of ischemic heart disease? *Hypertension* **38**: 1413–1415.
20. Weis, SM and Cheresh, DA (2005). Pathophysiological consequences of VEGF-induced vascular permeability. *Nature* **437**: 497–504.
21. Cao, Y, Hong, A, Schulten, H and Post, MJ (2005). Update on therapeutic neovascularization. *Cardiovasc Res* **65**: 639–648.
22. Adams, RH and Alitalo, K (2007). Molecular regulation of angiogenesis and lymphangiogenesis. *Nat Rev Mol Cell Biol* **8**: 464–478.
23. Jenkins, MJ, Edgley, AJ, Sonobe, T, Umetani, K, Schwenke, DO, Fujii, Y *et al.* (2012). Dynamic synchrotron imaging of diabetic rat coronary microcirculation in vivo. *Arterioscler Thromb Vasc Biol* **32**: 370–377.
24. Iwasaki, H, Fukushima, K, Kawamoto, A, Umetani, K, Oyamada, A, Hayashi, S *et al.* (2007). Synchrotron radiation coronary microangiography for morphometric and physiological evaluation of myocardial neovascularization induced by endothelial progenitor cell transplantation. *Arterioscler Thromb Vasc Biol* **27**: 1326–1333.
25. Ludmer, PL, Selwyn, AP, Shook, TL, Wayne, RR, Mudge, GH, Alexander, RW *et al.* (1986). Paradoxical vasoconstriction induced by acetylcholine in atherosclerotic coronary arteries. *N Engl J Med* **315**: 1046–1051.
26. Marti, CN, Gheorghiade, M, Kalogeropoulos, AP, Georgiopoulou, VV, Quyyumi, AA and Butler, J (2012). Endothelial dysfunction, arterial stiffness, and heart failure. *J Am Coll Cardiol* **60**: 1455–1469.
27. Bonetti, PO, Lerman, LO and Lerman, A (2003). Endothelial dysfunction: a marker of atherosclerotic risk. *Arterioscler Thromb Vasc Biol* **23**: 168–175.
28. Poelzl, G, Frick, M, Huegel, H, Lackner, B, Alber, HF, Mair, J *et al.* (2005). Chronic heart failure is associated with vascular remodeling of the brachial artery. *Eur J Heart Fail* **7**: 43–48.
29. Meyer, B, Mörtl, D, Strecker, K, Hülsmann, M, Kulemann, V, Neunteufl, T *et al.* (2005). Flow-mediated vasodilation predicts outcome in patients with chronic heart failure: comparison with B-type natriuretic peptide. *J Am Coll Cardiol* **46**: 1011–1018.
30. Heitzer, T, Baldus, S, von Kodolitsch, Y, Rudolph, V and Meinertz, T (2005). Systemic endothelial dysfunction as an early predictor of adverse outcome in heart failure. *Arterioscler Thromb Vasc Biol* **25**: 1174–1179.

Figure S1

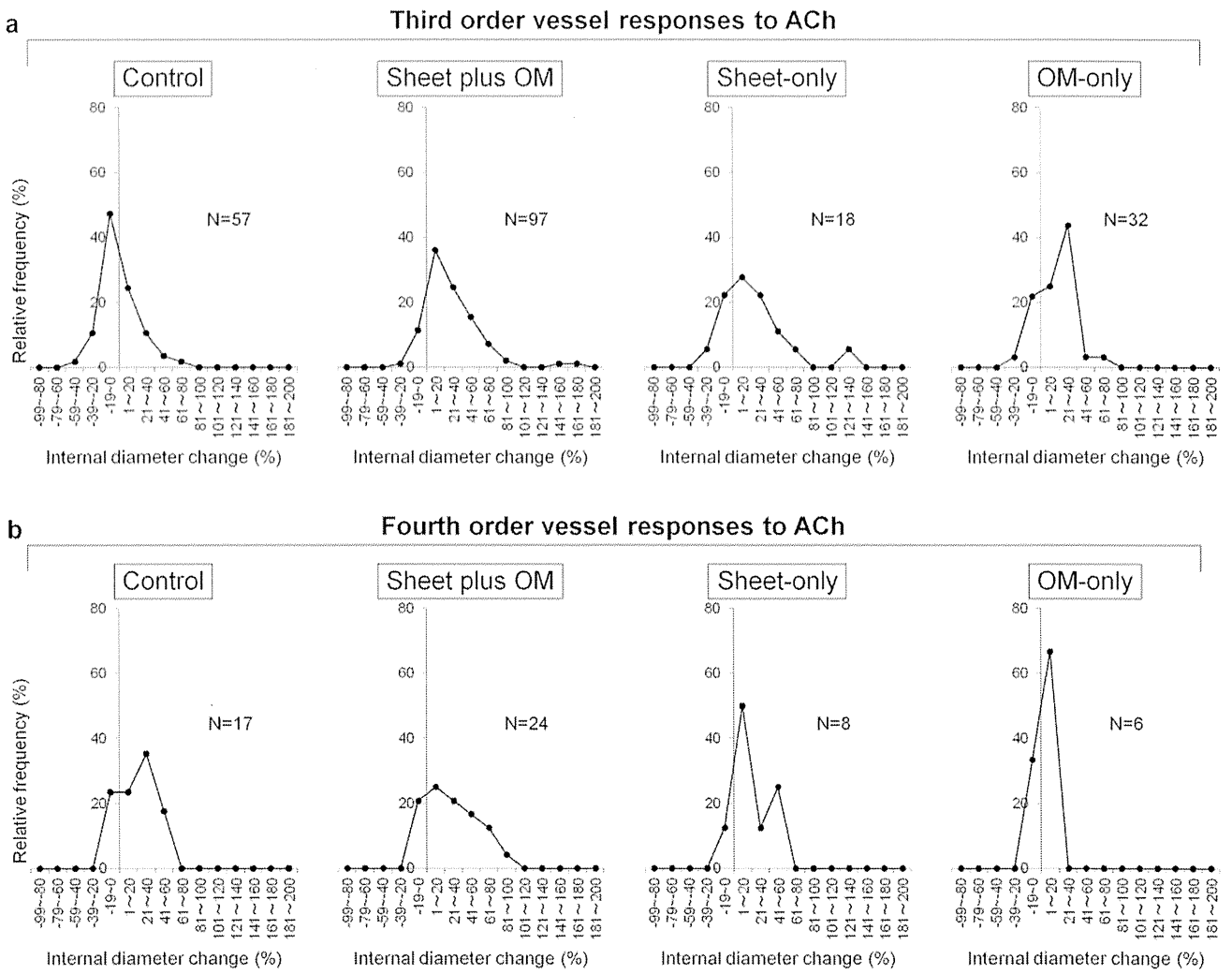
a
Third order vessel responses to ACh
Control
Sheet plus OM
Sheet-only
OM-only
N=57
N=97
N=18
N=32
Relative frequency (%)
Internal diameter change (%)
b
Fourth order vessel responses to ACh
Control
Sheet plus OM
Sheet-only
OM-only
N=17
N=24
N=8
N=6
Relative frequency (%)
Internal diameter change (%)